Infrared-to-visible upconversion processes in Pr^{3+}/Yb^{3+}-codoped KPb_2Cl_5

R. Balda,[1,2,3] J. Fernández,[1,2,3] A. Mendioroz,[1] M. Voda,[1] and M. Al-Saleh[1]
[1]*Departamento Fisica Aplicada I, Escuela Superior de Ingenieros, Alda. Urquijo s/n 48013 Bilbao, Spain*
[2]*Centro Mixto CSIC-UPV/EHU, Basque Country, Spain*
[3]*Donostia International Physics Center (DIPC), Basque Country, Spain*
(Received 13 May 2003; revised manuscript received 29 July 2003; published 10 October 2003)

In this work we report infrared-to-visible upconversion luminescence in the low-phonon-energy host material KPb_2Cl_5 codoped with Pr^{3+} and Yb^{3+} ions. An orange luminescence from the $^1D_2$ level, and less intense blue, green, and red emissions from the $^3P_{0,1}$ levels of Pr^{3+} have been observed under resonant excitation in the $^1G_4$ level of Pr^{3+}. As regards to Yb^{3+}, when the $^2F_{5/2}$ level is resonantly excited, the visible emissions are also present but the blue, green, and red emissions from $^3P_{0,1}$ levels are enhanced if compared with the orange luminescence from level $^1D_2$. On the other hand, excitation at the high-energy wing of the $^2F_{5/2}$ level originates emission only from $^3P_{0,1}$ levels. The upconverted fluorescence from the $^1D_2$ and $^3P_{0,1}$ levels occurs by energy transfer upconversion and/or excited-state absorption processes depending on the excitation wavelength. The possible mechanisms which lead these processes are discussed.

DOI: 10.1103/PhysRevB.68.165101 PACS number(s): 78.20.−e, 78.55.Hx, 42.70.Hj, 42.65.Ky

I. INTRODUCTION

Frequency upconversion of infrared (IR) into visible (VIS) light in rare-earth- (RE-) doped solids has been investigated intensively due to the possibility of infrared-pumped visible lasers and their potential applications such as color display, optical storage, optoelectronics, and medical applications. Recently, the search for all-solid compact laser devices operating in the blue-green region and the availability of powerful near-infrared laser diodes have increased the interest in upconversion emission. Among rare-earth ions, trivalent praseodymium is an attractive optical activator which offers the possibility of simultaneous blue, green, and red emission for laser action as well as IR emission for optical amplification at 1.3 μm. Pr^{3+} systems are also interesting as short-wavelength upconversion laser materials. Laser operation using single and double infrared pumped configurations has already been demonstrated in praseodymium doped systems.[1–5] The trivalent praseodymium ground-state $^3H_4$ to $^1G_4$ transition is spin forbidden, which implies weak pump absorption in the spectral region around 1 μm, where high-power sources are commercially available. The sensitization of rare-earth-doped materials with Yb^{3+} ions is a well-known method for increasing the optical pumping efficiency because of the efficient energy transfer from Yb^{3+} to rare-earth ions. The use of trivalent ytterbium to populate the $^1G_4$ level of Pr^{3+} ions has been proposed for applications to 1.3 μm (Ref. 6) and upconversion (Ref. 1) lasers. The high-absorption cross section of ytterbium ions around 980 nm and the possibility of an efficient energy transfer mechanism between rare-earth ions can improve the upconversion efficiency in ytterbium-sensitized Pr^{3+} systems.[7–11] Moreover, the broad absorption band of Yb^{3+} ions allows one to use a wide range of excitation wavelengths with higher absorption cross sections than in the case of single Pr^{3+}-doped systems.

In order to investigate new upconversion materials with high luminescence efficiency, hosts with low phonon energies are required. The low phonon energy leads to low nonradiative transition rates due to multiphonon relaxation and high radiative transition rates, which increase the quantum efficiency from excited states of active ions. Sulfide- and chloride-based hosts have been studied as their phonon energies are lower than in fluoride crystals. However, these materials usually present poor mechanical properties and moisture sensitivity, and are difficult to synthesize. Recently, KPb_2Cl_5 crystal has been studied as a promising host for RE ions[12–16] because it is nonhygroscopic and readily incorporates rare-earth ions. The crystal is biaxial, crystallizes in the monoclinic system[17] (space group $P2_1/c$) with lattice parameters $a=0.8831$ nm, $b=0.7886$ nm, $c=1.243$ nm, and $\beta=90.14°$, and it is transparent in the 0.3–20 μm spectral region. According to Raman-scattering measurements the maximum phonon energy of optical phonons for this crystal is equal to 203 cm^{-1}. Spectroscopic and lasing investigations of this crystal doped with Dy^{3+} ions suggest that Dy^{3+} substitutes Pb^{2+} ions and K^+ vacancies are assumed to provide charge compensation.[14]

In a preliminary work, the authors have shown the existence of infrared-to-visible upconversion in a single Pr^{3+}-doped KPb_2Cl_5 crystal.[18] In the present work we report a spectroscopic study of the infrared-to-visible luminescence of Pr^{3+} ions in Pr^{3+}/Yb^{3+}-codoped KPb_2Cl_5 crystals. We study the upconversion luminescence of Pr^{3+} upon continuous wave (cw) excitation in the $^1G_4$ level of Pr^{3+} ions and/or in the $^2F_{7/2}\rightarrow{}^2F_{5/2}$ absorption band of ytterbium ions. Resonant excitation of the $^2F_{5/2}$ and/or $^1G_4$ levels leads to orange fluorescence from the $^1D_2$ state together with blue, green, and red emissions from the $^3P_{0,1}$ levels, whereas excitation in the high-energy wing of the $^2F_{7/2}\rightarrow{}^2F_{5/2}$ absorption band of Yb^{3+} originates emission only from $^3P_{0,1}$ levels. As we shall see, this latter upconversion emission can be attributed to a sequential two-photon absorption in which the excited Yb^{3+} ion transfers its energy to the $^1G_4$ level of the Pr^{3+} ion and then a second IR photon is absorbed which allows the electronic transition to the $^3P_0$ level. However, under resonant pumping of the $^2F_{5/2}$ manifold the mechanism to populate the $^3P_{0,1}$ levels is a three-photon energy transfer upconversion (ETU) process. It is worthy to notice that codoping with Yb^{3+} ions allows us to select the upcon-

version emission only from levels $^3P_{0,1}$ by tuning of the excitation wavelength. The upconverted orange emission from level $^1D_2$ shows a quadratic dependence on the pump power which points to a two-photon process. This level is populated by ETU and/or excited-state absorption (ESA) depending on the excitation wavelength.

II. EXPERIMENTAL TECHNIQUES

Single crystals of nonhygroscopic ternary potassium-lead chloride KPb_2Cl_5 doped with Pr^{3+} ions and codoped with Pr^{3+} and Yb^{3+} ions, typically 3 cm long and 2 cm in diameter, have been grown in our laboratory by the Bridgman technique, in a chlorine atmosphere with a two-zone transparent furnace, a vertical temperature gradient of 18 °C/cm, and a 1-mm-per-hour growth rate. Quartz ampoules with a pointed end were used as seed selectors to promote single-crystal growth. The pure crystals are transparent and colourless. The Pr^{3+} and Yb^{3+} content did not exceed 0.5 mol % in the melt. The plates with approximate dimensions of $10\times6\times3$ mm^3 were cut from blocks and adequately polished for spectroscopic measurements.

The samples temperature was varied between 4.2 K and 300 K with a continuous-flow cryostat. Conventional absorption spectra between 175 nm and 3000 nm were performed with a Cary 5 spectrophotometer. The steady-state emission measurements were made with an argon laser and a Ti-sapphire ring laser (0.4 cm^{-1} linewidth) in the 920–1060 nm range as exciting light. The fluorescence was analyzed with a 0.25-m monochromator, and the signal was detected by a Hamamatsu R928 photomultiplier and finally amplified by a standard lock-in technique. For the fluorescence dynamic measurements a digital oscilloscope was used to record the decay and rise signals.

III. RESULTS

Figure 1 shows the absorption coefficient as a function of wavelength in the 400–2500 nm range at room temperature for the codoped sample. It consists of several bands corresponding to transitions between the $^3H_4$ ground state and the excited multiplets belonging to the $4f^2$ configuration of Pr^{3+} ions together with the broad band corresponding to the $^2F_{7/2}\rightarrow{}^2F_{5/2}$ transition of Yb^{3+} ions between 900 and 1100 nm. Figure 2 shows the absorption coefficient of the single-doped and codoped samples with the same Pr^{3+} concentration between 900 and 1100 nm. The absorption band corresponding to the $^3H_4\rightarrow{}^1G_4$ transition of Pr^{3+} lies in the same spectral range but its absorption cross section is one order of magnitude smaller than in the $^2F_{7/2}\rightarrow{}^2F_{5/2}$ transition of Yb^{3+} ions.

Figure 3 shows the room-temperature steady-state emission spectrum obtained under one photon (OP) excitation at 454 nm together with the upconverted emission spectra obtained at room temperature by exciting at different wavelengths along the $^2F_{7/2}\rightarrow{}^2F_{5/2}$ absorption band of Yb^{3+} ions. As can be seen in Fig. 3(a), after excitation in the $^3P_2$ level (454 nm) the emission corresponds to levels $^3P_0$ and $^3P_1$. The spectrum consists of several lines corresponding to

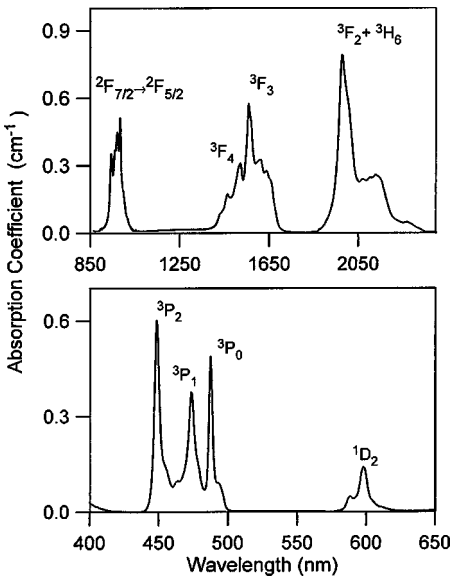

FIG. 1. Room-temperature absorption spectrum in the visible and near-infrared regions in the codoped crystal.

transitions $^3P_0\rightarrow{}^3H_{4,5,6}$, $^3P_0\rightarrow{}^3F_{2,3,4}$ and $^3P_1\rightarrow{}^3H_{4,5,6}$, $^3P_1\rightarrow{}^3F_{2,3,4}$. As expected, due to the energy gap between the $^3P_0$ and $^1D_2$ levels (3560 cm^{-1}) and to the low phonon energy involved (203 cm^{-1}), no fluorescence emission from level $^1D_2$ occurs. Figure 3(b) shows the room-temperature emission spectrum obtained by exciting at 1018 nm. At this wavelength the Yb^{3+} and Pr^{3+} ions are simultaneously excited. As can be observed, after infrared excitation, there is emission from levels $^3P_{0,1}$ and $^1D_2$, and the spectrum is similar to the one obtained in a single-doped Pr^{3+} sample. When the excitation is performed in the highest-intensity Stark component of the $^2F_{7/2}\rightarrow{}^2F_{5/2}$ absorption band of ytterbium ions at 983 nm, Fig. 3(c), the spectrum shows similar features with an enhancement of the emission from levels $^3P_{0,1}$. However, the spectrum obtained under excitation at the high-energy side of the ytterbium absorption band at 937.5 nm shows emission only from levels $^3P_{0,1}$. In this case [Fig. 3(d)] the upconversion emission spectrum is similar to the one obtained under OP excitation at 454 nm. It is important to note that at this excitation wavelength (937.5 nm) visible upconverted emission is not observed in the

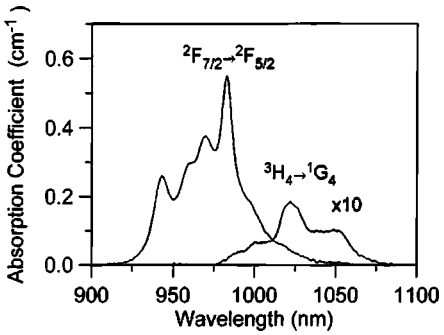

FIG. 2. Absorption coefficient of the single-doped and codoped samples with the same Pr^{3+} concentration between 900 and 1100 nm at room temperature.

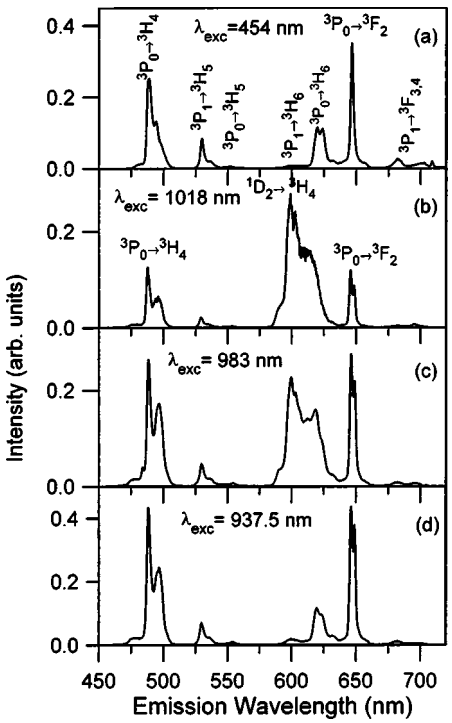

FIG. 3. Room temperature emission spectra obtained under excitation (a) at 454 nm, (b) at 1018 nm, (c) at 983 nm, and (d) at 937.5 nm in the codoped crystal.

single-doped crystal. However, for the codoped sample the upconversion emission is strong enough to be easily observed with the naked eye, which indicates the important role played by Yb^{3+} ions. A similar behavior is observed at low temperature.

To investigate the excitation mechanisms for populating the $^3P_{0,1}$ and $^1D_2$ levels after IR excitation, we have obtained the dependence of the upconverted emission intensities for different pumping powers. The upconversion emission intensity (I_{em}) depends on the incident pump power (P_{pump}) according to the relation $I_{em} \propto (P_{pump})^n$, where n is the number of photons involved in the pumping mechanism. Figure 4 shows a logarithmic plot of the integrated emission intensity of the upconverted fluorescence at 489 nm ($^3P_0$)

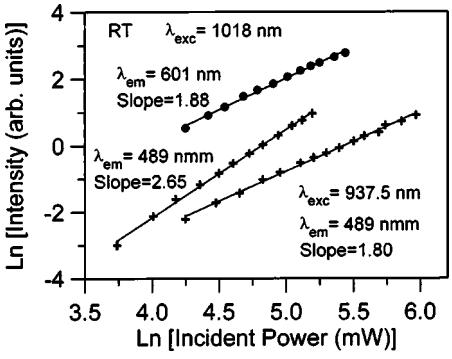

FIG. 4. Logarithmic plot of the integrated intensities of the upconverted emission from $^3P_0$ (489 nm) and $^1D_2$ (601 nm) levels in the codoped crystal obtained under IR excitation at different wavelengths.

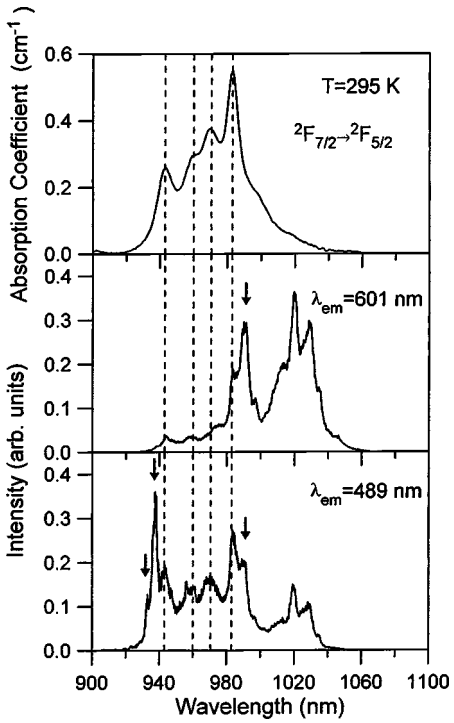

FIG. 5. Excitation spectra of the upconverted emission from $^3P_0$ (489 nm) and $^1D_2$ (601 nm) levels obtained in the codoped crystal at 295 K, corrected for the spectral variation of the laser intensity. The one-photon absorption spectrum is also included for comparison.

and 601 nm ($^1D_2$) as a function of the pump laser intensity obtained by exciting at 1018 nm and 937.5 nm. The dependence of the orange emission from level $^1D_2$ on the pump power shows a slope of 1.88 which indicates a two-photon upconversion process. However, the logarithmic plot of the blue emission shows a different behavior depending on the excitation wavelength. As can be seen in Fig. 4, under excitation at 1018 nm, it shows a roughly cubic behavior (slope 2.65) whereas under excitation at 937.5 nm it shows a nearly quadratic behavior, which indicates a two-photon process. It is worthy to notice that the cubic dependence of the blue emission on the pump power is always observed by exciting along the absorption band of Yb^{3+} ions except at the very-high-energy tail from 932 to 937.5 nm.

To further investigate the nature of the upconversion processes in this crystal, excitation spectra of the upconverted emissions at 489 and 601 nm were performed at 4.2 K, 77 K, and 295 K in the spectral range corresponding to the $^2F_{7/2} \rightarrow {}^2F_{5/2}$ and $^3H_4 \rightarrow {}^1G_4$ transitions of Yb^{3+} and Pr^{3+} ions, respectively. Figure 5 shows for comparison the room-temperature excitation spectra for the upconverted emissions of the codoped sample by monitoring the $^3P_0 \rightarrow {}^3H_4$ transition at 489 nm and the $^1D_2 \rightarrow {}^3H_4$ transition at 601nm together with the OP absorption spectrum. Important differences can be observed between the upconverted excitation spectra and the absorption spectrum. The spectra corresponding to the orange and blue emissions show two peaks around 1020 nm similar to those corresponding to the $^3H_4 \rightarrow {}^1G_4$ absorption band, four peaks at around 943, 960, 970, and 983

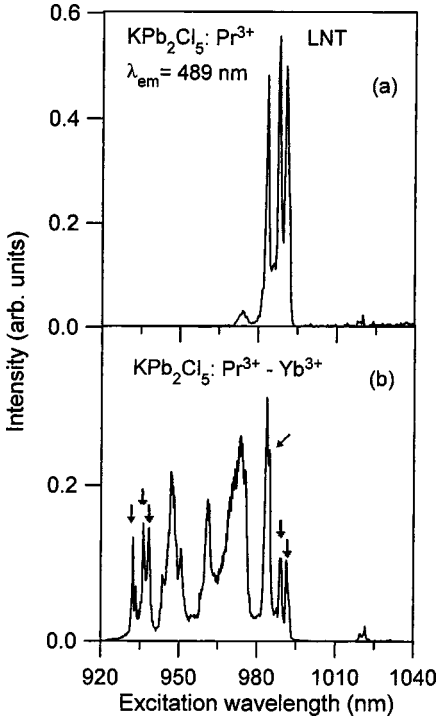

FIG. 6. Excitation spectra of the upconverted emission from $^3P_0$ (489 nm) level obtained at 77 K, corrected for the spectral variation of the laser intensity: (a) single-doped sample and (b) codoped sample.

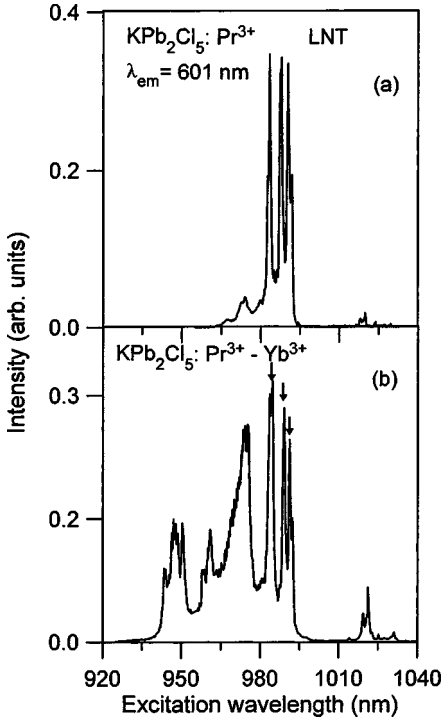

FIG. 7. Excitation spectra of the upconverted emission from the $^1D_2$ (601 nm) level obtained at 77 K, corrected for the spectral variation of the laser intensity: (a) single-doped sample and (b) codoped sample.

nm, which correspond to the main Stark components of the $^2F_{5/2}$ excited state of Yb^{3+} ions (marked by dashed lines), and some additional peaks not observed in the OP absorption spectrum indicated by arrows. These peaks appear at around 933, 937.5, and 990 nm in the excitation spectrum of the blue upconversion emission whereas the excitation spectrum of the orange emission from level $^1D_2$ only shows the peak at around 990 nm. Figures 6 and 7 show the excitation spectra of the blue and orange emission, respectively, obtained at 77 K for the single-doped and codoped crystals. In the case of the single-doped sample, the excitation spectra are similar for both blue and orange upconverted emission. These spectra present weak peaks similar to those corresponding to the $^3H_4 \rightarrow {}^1G_4$ absorption band of Pr^{3+} ions and strong excitation peaks around 983, 988, and 990 nm. In the codoped sample there is spectral overlap between the main Stark component of Yb^{3+} ion and the peak at 983 nm.

The temporal evolution of the upconversion luminescence was obtained in the codoped sample under chopped laser excitation at different wavelengths along the ytterbium absorption band. As an example, Fig. 8 shows the temporal behavior of the blue upconverted emission obtained under excitation at 937.5 nm in the high-energy side of the $^2F_{7/2} \rightarrow {}^2F_{5/2}$ absorption band and at 983 nm. As can be seen the decay times are different depending on the excitation wavelength.

The upconverted orange emission from level $^1D_2$ also shows different rise and decay times depending on the excitation wavelengths. Figure 9 shows the temporal behavior after excitation at 990 nm, which corresponds to the addi-

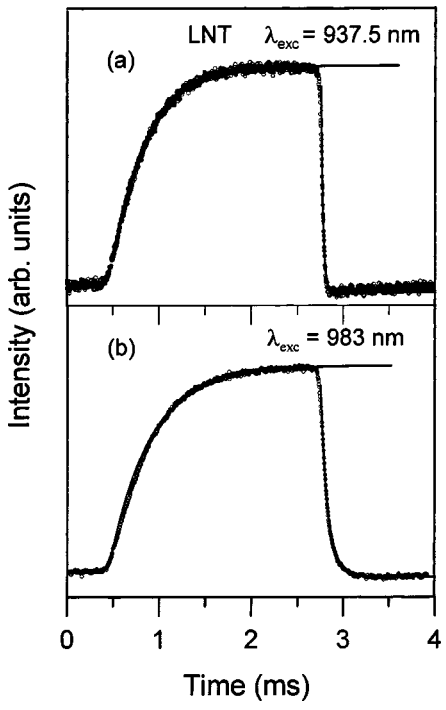

FIG. 8. Temporal behavior of the blue upconversion luminescence obtained at two different excitation wavelengths (a) 937.5 nm and (b) 983 nm in the codoped crystal. The experimental results are represented by the open circles. The solid line is the best fit to an exponential function. Data correspond to 77 K.

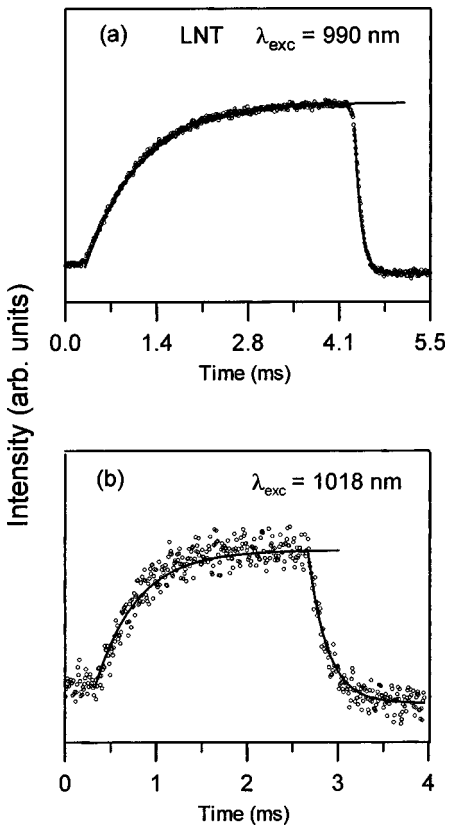

FIG. 9. Temporal behavior of the orange upconversion luminescence obtained at two different excitation wavelengths (a) 990 nm and (b) 1018 nm in the codoped crystal. The experimental results are represented by the open circles. The solid line is the best fit to an exponential function. Data correspond to 77 K.

tional peak found in the excitation spectrum and under excitation at 1018 nm (the barycenter of the $^3H_4 \rightarrow {}^1G_4$ absorption band).

The values of the rise and decay times obtained by fitting the experimental data to an exponential curve are displayed in Table I. As can be seen, under excitation at 937.5 nm, the lifetime of the blue emission is around 14 μs, which is close to the lifetime obtained under one photon excitation (11 μs).[15] The observed rise time is due to the long lifetime of state $^2F_{5/2}$ of Yb^{3+} (338 μs) which participates in the excitation process as an intermediate level. It is worthy to notice that the decay times obtained under excitation at 947, 960, and 983 nm are longer than the intrinsic decay time of the $^3P_0$ level. In the case of the orange emission from level $^1D_2$, the decay time obtained under excitation at 990 nm is close to the lifetime obtained under one-photon excitation (88 μs).[15] Under excitation at other wavelengths in resonance with the Stark components of Yb^{3+} ions or in resonance with the $^1G_4$ level the decay time is always longer than the intrinsic decay time of the $^1D_2$ level.

IV. DISCUSSION

A. Orange emission from the $^1D_2$ level

There are two basically different mechanisms to populate the $^1D_2$ level after infrared excitation: upconversion by energy transfer and excited-state absorption. In this system avalanche upconversion can be excluded, because none of the typical signatures for an avalanche process are observed. Excitation spectra of the upconverted luminescence provide a first possibility to distinguish between ESA and ETU mechanisms.[19,20] In the first mechanism a single ion is involved, whereas two ions are involved in the second one. In the case of ETU, the excitation spectrum is proportional to the square of the OP absorption coefficient as a function of wavelength whereas in the case of excited-state absorption the upconversion excitation spectrum is the result of OP absorption and excited-state absorption.

In our codoped sample since Yb^{3+} ions act as sensitizer, the intermediate $^1G_4$ state involved in the upconversion processes can be populated by energy transfer from a nearby excited Yb^{3+} ion and/or by direct $^3H_4 \rightarrow {}^1G_4$ absorption of Pr^{3+} ions. In accordance with these arguments, the excitation spectrum of the upconverted orange luminescence from level $^1D_2$ [Fig. 7(b)] shows the presence of the peaks corresponding to the $^2F_{7/2} \rightarrow {}^2F_{5/2}$ transition of Yb^{3+} ions besides the ones due to the $^3H_4 \rightarrow {}^1G_4$ transition of Pr^{3+} ions which clearly indicates that an Yb^{3+} to Pr^{3+} energy transfer as well as an ETU process from the $^1G_4$ multiplet takes place. However, this spectrum also presents additional intense peaks around 988 and 990 nm the energies of which are resonant with the $^3F_{3,4} \rightarrow {}^1D_2$ transitions. The intermediate $^3F_4$ level required for this ESA process can be populated by (i) multiphonon relaxation or (ii) cross relaxation of the $^1G_4 \rightarrow {}^3H_5$ and $^3H_4 \rightarrow {}^3F_4$. Due to the energy gap between $^1G_4$

TABLE I. Rise and decay times of the blue (489 nm) and orange (601 nm) upconversion luminescence obtained at different excitation wavelengths at 77 K in the codoped crystal.

$\lambda_{em} = 489$ nm						
λ_{exc}	937.5 nm	947 nm	960 nm	983 nm	990 nm	1018 nm
Rise (μs)	392	454	450	430	—	—
Decay (μs)	14	85	95	76	—	—
$\lambda_{em} = 601$ nm						
λ_{exc}	937.5 nm	947 nm	960 nm	983 nm	990 nm	1018 nm
Rise (μs)	—	473	466	568	825	367
Decay (μs)	—	211	217	172	100	210

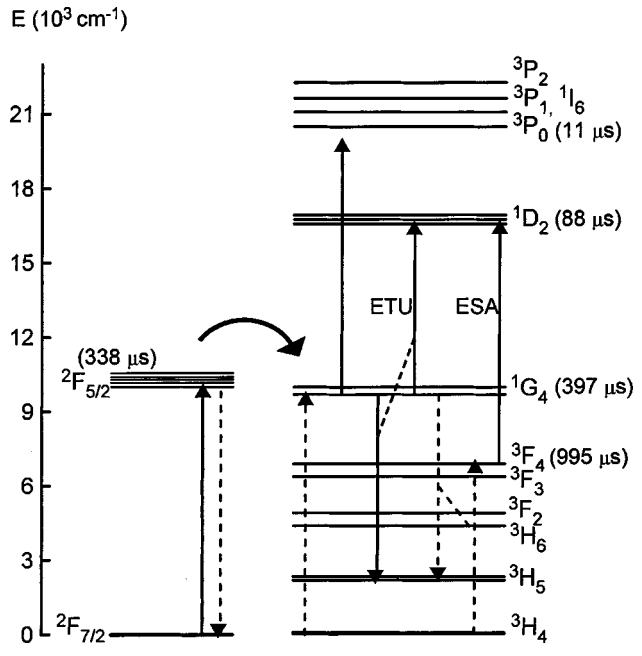

FIG. 10. Energy level diagram of Pr^{3+}-Yb^{3+} in KPb_2Cl_5 crystal and the possible upconversion mechanisms to populate the $^1D_2$ level after IR excitation.

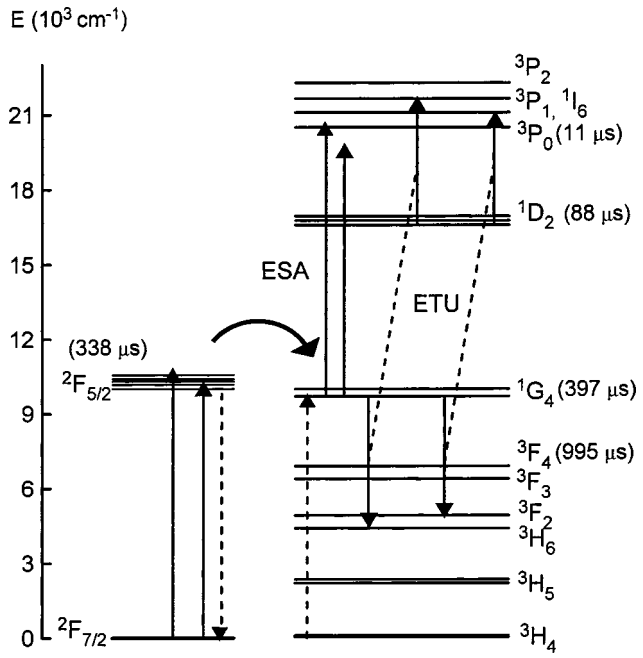

FIG. 11. Energy level diagram of Pr^{3+}-Yb^{3+} in KPb_2Cl_5 crystal and the possible upconversion mechanisms to populate the $^3P_0$ level after IR excitation.

and $^3F_4$ levels ($\approx 3200\ cm^{-1}$) and the phonon energies involved ($203\ cm^{-1}$), cross relaxation of level $^1G_4$ seems to be the most likely mechanism to populate the $^3F_4$ level.

In conclusion, as shown in the level diagram of Fig. 10, both ETU and ESA processes do contribute to the observed upconversion luminescence from the $^1D_2$ level. These results are further confirmed by lifetime measurements. As can be seen in Table I the decay time of the upconverted luminescence obtained by exciting at the ESA peaks is close to the OP direct excitation of the $^1D_2$ level (88 μs), whereas for the remaining wavelengths along the excitation spectrum, the decay times are longer ($\cong 210\ \mu s$) than the intrinsic decay time of the level which indicates the presence of ETU processes. The longer values of the decays which are about half the lifetime of the $^1G_4$ state (397 μs) suggest that the $^1D_2$ level is populated by an ETU processes involving two Pr^{3+} ions in the $^1G_4$ level ($^1G_4$, $^1G_4$)$\rightarrow$($^1D_2$, $^3H_5$).

The rise time observed under excitation at the ESA peaks, which is longer than those obtained by exciting at other wavelengths along the $^2F_{7/2}\rightarrow{}^2F_{5/2}$ absorption of Yb^{3+} ions and at the $^3H_4\rightarrow{}^1G_4$ transition of Pr^{3+} ions, indicates that the $^1D_2$ level is being fed by upconversion from the long-lived $^3F_4$ level (995 μs).

Finally, it is worth noticing that as shown in Fig. 7(a), in the case of the single-doped sample, the ESA mechanism is the most important one for populating level $^1D_2$ at low temperatures.

B. Blue emission from the $^3P_0$ level

As we have shown in Fig. 6(b), the excitation spectrum of the blue upconverted luminescence shows some similar features with the one obtained for the orange upconverted emission. However, together with the peaks corresponding to the absorption of Yb^{3+} ions and the small features corresponding to the direct $^3H_4\rightarrow{}^1G_4$ transition of Pr^{3+} ions, other peaks appear above and below the $^2F_{5/2}$ manifold of Yb^{3+} ions. As depicted in Fig. 11, the peaks above the manifold of the excited state of Yb^{3+} ions around 933 and 937.5 nm may be due to an ESA process produced by the $^1G_4\rightarrow{}^3P_0$ excited-state absorption. This hypothesis is confirmed by the results gathered in Fig. 4 where we have shown that under excitation at the high-energy wing of the Yb^{3+} absorption band the blue emission from level $^3P_0$ presents a quadratic dependence on pumping power which indicates a two-photon process. In this case, in a first step the absorption of one IR photon excites the Yb^{3+} ions to the $^2F_{5/2}$ level then the excited Yb^{3+} ion transfers its energy to a Pr^{3+} ion and excites it to level $^1G_4$. Then the absorption of a second IR photon excites the Pr^{3+} ion from level $^1G_4$ to $^3P_0$. Moreover, when these peaks are excited, the decay time of the blue emission is similar to the intrinsic decay time of this level which confirms the presence of an ESA process. This two-photon upconversion process is only observed in the codoped sample.

As shown in the level diagram of Fig. 11, for the excitation energies corresponding to the remaining peaks of the excitation spectrum of the blue upconverted luminescence (i.e., resonant excitation of levels $^2F_{5/2}$ and/or $^1G_4$ which leads to the upconverted emissions from levels $^3P_{0,1}$ and $^1D_2$) there is not enough energy to populate the $^3P_0$ level by a sequential two-photon process. In this case, the $^3P_0$ population roughly behaves as the third power (2.65) of cw laser excitation, which implies either ETU processes involving three ions or stepwise absorption of three photons via nonresonant absorption.[21,22] On the other hand, the features of

the excitation spectrum of the blue upconversion emission around 990 nm are similar to the ones found in the single-doped sample [Fig. 6(a)] and in the orange upconversion from the $^1D_2$ multiplet which reveals the participation of this level in the blue upconversion process through the above-mentioned $^3F_{3,4} \rightarrow {}^1D_2$ transitions. Moreover, the time evolution of the upconverted blue emission gives further evidences that an ETU involving the $^1D_2$ level can be responsible for the upconversion emission from the $^3P_0$ level since the decay times obtained under excitation at 947, 960, and 983 nm are much longer than the intrinsic decay time of the $^3P_0$ level. According to the energy level diagram in Fig. 11, there exist several resonances such as $^1G_4 \rightarrow {}^3H_6$ with $^1D_2 \rightarrow {}^1I_6$ and $^1G_4 \rightarrow {}^3F_2$ with $^1D_2 \rightarrow {}^3P_1$ that can lead to a quasicubic power dependence of the upconversion fluorescence intensity.

V. CONCLUSIONS

IR-to-visible upconversion in Pr^{3+}-Yb^{3+}-codoped KPb_2Cl_5 low phonon crystal has been investigated under continuous-wave laser excitation in the range from 900 to 1100 nm. Resonant excitation of the $^2F_{5/2}$ and/or $^1G_4$ levels leads to an orange emission from the $^1D_2$ level, together with blue, green, and red lines from the $^3P_{0,1}$ levels. The features of the excitation spectra of the upconverted luminescence from level $^1D_2$ together with its quadratic dependence on the pumping power and time evolution suggest that ETU and ESA upconversion mechanisms involving praseodymium ions in the intermediate $^3F_{3,4}$ states are responsible for the upconverted luminescence from this level. Concerning the emission from $^3P_{0,1}$ levels, the roughly cubic (2.65) dependence on the pump power of the blue emission points out to a three-photon mechanism involving the $^1D_2$ state.

It is worthy to notice that excitation at the high-energy wing of the Yb^{3+} absorption band leads only to emission from levels $^3P_{0,1}$ not observable in the single-doped crystal. In this case, the pumping power dependence of the blue emission is quadratic which indicates a two-photon process to populate these levels. The features of the excitation spectra of the blue emission together with its temporal evolution point to an ESA upconversion mechanism as being responsible for this upconversion.

Finally, it is important to notice that by codoping KPb_2Cl_5 crystal with Yb^{3+}-Pr^{3+} ions we are able to select the upconversion emitting level by an adequate tuning of the excitation wavelength.

ACKNOWLEDGMENTS

This work was supported by the Spanish Government MCYT (Grant No. BFM2000-0352), Basque Country Government (Grant No. PI-1999-95), and Basque Country University (Grant No. UPV13525/2001).

[1] J.Y. Allain, M. Monerie, and H. Poignant, Electron. Lett. **27**, 1156 (1991).
[2] R.G. Smart, D.C. Hanna, A.C. Tropper, S.T. Davey, S.F. Carter, and D. Szebesta, Electron. Lett. **27**, 1307 (1991).
[3] T. Sandrock, H. Scheife, E. Heumann, and G. Huber, Opt. Lett. **22**, 808 (1997).
[4] Y. Zhao and S. Poole, Electron. Lett. **30**, 967 (1994).
[5] D.M. Baney, G. Rankin, and K.W. Chang, Opt. Lett. **21**, 1372 (1996).
[6] J.Y. Allain, M. Monerie, and H. Poignant, Electron. Lett. **27**, 1012 (1991).
[7] D. Piehler, D. Craven, N. Kwong, and H. Zarem, Electron. Lett. **29**, 1857 (1993).
[8] D.M. Baney, L. Yang, J. Ratcliff, and K.W. Chang, Electron. Lett. **31**, 1842 (1995).
[9] D.M. Baney, G. Rankin, and K.W. Chang, Appl. Phys. Lett. **69**, 1662 (1996).
[10] T.R. Gosnell, Electron. Lett. **33**, 411 (1997).
[11] W. Lozano B., Cid B. De Araujo, C. Egalon, A.S.L. Gomes, B.J. Costa, and Y. Messaddeq, Opt. Commun. **153**, 271 (1998).
[12] M.C. Nostrand, R.H. Page, S.A. Payne, W.F. Krupke, P.G. Schunemann, and L.I. Isaenko, OSA Trends Opt. Photonics Ser. **19**, 524 (1998).
[13] M.C. Nostrand, R.H. Page, S.A. Payne, W.F. Krupke, P.G. Schunemann, and L.I. Isaenko, OSA Trends Opt. Photonics Ser. **26**, 441 (1999).
[14] M.C. Nostrand, R.H. Page, S.A. Payne, L.I. Isaenko, and A.P. Yelisseyev, J. Opt. Soc. Am. B **18**, 264 (2001).
[15] R. Balda, M. Voda, M. Al-Saleh, and J. Fernández, J. Lumin. **97**, 94 (2002).
[16] A. Mendioroz, J. Fernández, M. Voda, M. Al-Saleh, A.J. Garcia-Adeva, and R. Balda, Opt. Lett. **27**, 1525 (2002).
[17] K. Nitsch, M. Dusek, M. Nikl, K. Polák, and M. Rodová, Prog. Cryst. Growth Charact. Mater. **30**, 1 (1995).
[18] R. Balda, J. Fernández, A. Mendioroz, M. Voda, and M. Al-Saleh, Opt. Mater. (to be published).
[19] F. Auzel, Proc. IEEE **61**, 758 (1973).
[20] J.C. Wright, Top. Appl. Phys. **15**, 239 (1976).
[21] M. Malinowski, M.F. Joubert, and B. Jacquier, Phys. Rev. B **50**, 12 367 (1994).
[22] A. Remillieux and B. Jacquier, J. Lumin. **68**, 279 (1996).